

Electron scattering and conduction in doped semiconductors in simultaneous strong infrared radiation field

I. F. Barna and S. Varró

*Wigner Research Centre for Physics of the Hungarian Academy of Sciences,
Konkoly - Thege Miklós út 29 - 33,*

*1121 Budapest, Hungary
and*

*ELI-HU Nonprofit Kft.,
Dugonics Tér 13, 6720 Szeged, Hungary*

(Dated: December 14, 2024)

Electron scattering and conduction on various types of impurities in semiconductor can be calculated via the first order Born approximation when the electrons are considered as free particles described by plane waves. In the following we present analytic angular differential cross section formula for electromagnetic radiation field assisted electron scattering on impurities approximated with various model potentials in semiconductors. The main idea describes the scattering electrons with the well-known Volkov wave function which automatically incorporates electron dynamics induced by the external oscillating field. This description is well-known for strong laser fields from half a century. The calculated electron conductance in the semiconductor could be enhanced with an order of magnitude if an infrared electromagnetic field is present with $I = 10^{14}$ W/cm² intensity, which for instance will be achievable in the ELI-ALPS facility in the near future.

PACS numbers: 61.82.Fk, 72.20.-i, 72.20.Dp, 32.80.Wr

I. INTRODUCTION

The discovery of semiconductors initiated an enormous development on electronic engineering and on everyday life. Developing newer and newer type of semiconductor devices with various conduction properties is an evergreen hot topic as well. The existing literature is therefore enormous, and the basics physics of semiconductors can be found in numerous textbooks like [1–4].

To investigate the electric conduction of semiconductors the key issue is to study scattering processes of electrons on impurities. The rate of transition probabilities of the scattering process can be derived from the one-electron time-dependent Schrödinger equation with the help of the first Born approximation.

Different models exist to approximate the electron-impurity potential scattering interaction via a central potential of $U(r)$. The part dealing with this issue of our present paper usually investigated in solid state physics.

As a new feature we extend this kind of modeling where an electromagnetic (EM) field is simultaneously present with infrared carrier frequencies therefore the main motivation of this investigation come from the fields of laser physics.

Nowadays optical laser intensities exceeded the 10^{22} W/cm² limit where radiation effects dominate the electron dynamics [5]. In the field of laser-matter interaction a large number of non-linear response of atoms, molecules and plasmas can be investigated both theoretically and experimentally. Such interesting high-field phenomena are high harmonic generations, or plasma-based laser-electron acceleration. This field intensities open the door to high field quantum electrodynamics phenomena like vacuum-polarization effects of pair production [5]. The original theory of potential scattering in external EM fields was developed about half a century ago and can be found in various papers of [6–13]. Numerous surveys on laser assisted electron collisions on atoms are available as well [14]. Kanya and Yamanouchi generalized the Kroll-Watson formula [15] for a single-cycle infrared pulse and applied it to time-dependent electron diffraction. There are only two studies available where heavy particles like protons scatter on nuclei in strong electromagnetic fields [16, 17]. Theoretical studies of solid states in such strong electromagnetic fields are rare. In the last years it became possible to investigate the band-gap dynamics [18] later the strong-field resonant dynamics [19] of semiconductors in the attosecond (as) time scale.

In the following we give self-contained overview of electron conduction calculation in a doped semiconductor, theory of laser assisted potential scattering, and numerical calculation of Lindhard dielectric function which are all essential tools for the presented theoretical description.

Finally, we present numerical calculation for model potential in infrared electromagnetic fields with intensities of magnitude of $I = 10^{14}$ W/cm². The photon energy of such fields are below 1eV which is comparable to some semiconductor band gaps. Our investigation shows that electrical conductivity of doped semiconductors can be enhanced with a factor of ten in some cases which may open the way to a new kind of gating. These kind of coherent infrared radiations will be soon available, for example in the Hungarian ELI-ALPS Laser Facility in Szeged [20].

II. THEORY

A. Electron scattering on impurities in semiconductors

For a better understanding of the whole formalism we give a short overview how the electron conductivity can be derived from first quantum mechanical and statistical physical principles. A much detailed derivation can be found in many theoretical solid state physics textbooks like [1–4].

Consider free electrons in two dimensions. Define the initial and final states to be plane waves of the form of

$$\varphi_i(\mathbf{r}) = \frac{A}{(2\pi\hbar)^{3/2}} \exp\left(\frac{i}{\hbar} \mathbf{p}_i \cdot \mathbf{r}\right), \quad \varphi_f(\mathbf{r}) = \frac{A}{(2\pi\hbar)^{3/2}} \exp\left(\frac{i}{\hbar} \mathbf{p}_f \cdot \mathbf{r}\right). \quad (1)$$

The perturbation is simply the extra potential energy of the impurity $U(\mathbf{r})$, so the transition rates are

$$U_{fi} = \int \varphi_f(\mathbf{r})^* U(\mathbf{r}) \varphi_i(\mathbf{r}) d\mathbf{r} = \frac{1}{A} \int U(\mathbf{r}) e^{-i\mathbf{q}\cdot\mathbf{r}} d^2\mathbf{r}, \quad (2)$$

which is simply the two-dimensional Fourier transform of the scattering potential. Note, that $\mathbf{q} = \mathbf{p}_i - \mathbf{p}_f$ is the momentum transfer of the scattering electron. The differential Born cross section of the corresponding potential is given by: $\frac{d\sigma_B}{d\Omega} = \left(\frac{m}{2\pi\hbar^2}\right)^2 |U(\mathbf{q})|^2$.

The well-known total scattering cross section σ_T for the elastic process can be calculated from the differential scattering cross section via an angular integration, where the back scattered electrons gives significant contributions therefore the $[1 - \cos(\theta)]$ appears

$$\sigma_T = 2\pi \int_0^\pi \left(\frac{d\sigma_B(\theta)}{d\Omega}\right) [1 - \cos(\theta)] \sin(\theta) d\theta. \quad (3)$$

The relaxation time τ single-particle life time (against impurity scattering, to be precise) is defined in terms of the total scattering cross section by multiplying with the number of impurities n_{imp}

$$1/\tau = \sigma_T n_{imp}. \quad (4)$$

Finally the electron mobility and the conductivity is defined via the following two formulas

$$\mu = e\tau/m^*, \quad G = e\mu n_e \quad (5)$$

where e, m^*, n_e are the elementary charge, effective mass and the number of the scattered electrons, respectively.

Further technical details including references and an overview over various methods (eg. Eq. (3) can be derived from the Boltzmann equation as well) are given in the review by Chattopadhyay [21].

B. Electromagnetic field assisted potential scattering

To have a self-constraint study we summarize our applied non-relativistic quantum mechanical description in some details. The coherent infrared field is treated semi-classically via the minimal coupling. The beam is taken to be linearly polarized and the dipole approximation is used. If the dimensionless intensity parameter (or the normalized vector potential) $a_0 = 8.55 \cdot 10^{-10} \sqrt{I(\frac{W}{cm^2})} \lambda(\mu m)$ of the external field is smaller than unity the non-relativistic description in dipole approximation is valid. For 800 nm laser wavelength this means a critical intensity of $I = 2.13 \cdot 10^{18} W/cm^2$, however we shall assume much smaller intensities.

Additionally, we consider moderate electron kinetic energy below one eV.

To describe the non-relativistic scattering process of a the electron on an impurity by a spherically symmetric external field the following Schrödinger equation has to be solved,

$$\left[\frac{1}{2m} \left(\hat{\mathbf{p}} - \frac{e}{c} \mathbf{A} \right)^2 + U(\mathbf{r}) \right] \Psi = i\hbar \frac{\partial \Psi}{\partial t}, \quad (6)$$

where $\hat{\mathbf{p}} = -i\hbar\partial/\partial\mathbf{r}$ is the momentum operator of the electron, and $U(\mathbf{r})$ represents the scattering potential of the impurity atom, $\mathbf{A}(t) = A_0 \mathbf{e} \cos(\omega t)$ is the vector potential of the radiation field with unit polarization vector \mathbf{e} . In Figure 1 we present the scattering geometry. The \mathbf{p}_i and \mathbf{p}_f are the initial and final electron momenta, θ is the

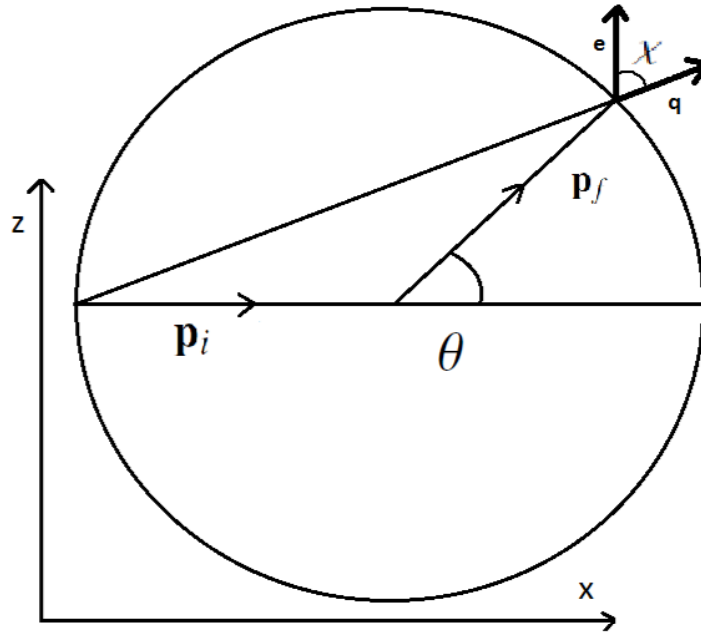


FIG. 1: The geometry of the scattering process. The impurity atom is in the center of the circle, \mathbf{p}_i and \mathbf{p}_f stand for the initial and final scattered electron momenta, θ is the electron scattering angle, the EM pulse propagates parallel to the x axis and linearly polarized in the x-z plane. The χ angle is needed for calculating the EM-electron momentum transfer.

scattering angle of the electron, the EM field is linearly polarized in the x-z plane, and the propagation of the EM field is parallel to the x axis.

Without the external scattering potential $U(\mathbf{r})$ the particular solution of (6) can be immediately written down as non-relativistic Volkov states $\varphi_p(\mathbf{r}, t)$ which exactly incorporate the interaction with the EM field,

The Volkov states, are modulated de Broglie waves, parametrized by momenta \mathbf{p} and form an orthonormal and complete set

$$\varphi_p(\mathbf{r}, t) = \frac{1}{(2\pi\hbar)^{3/2}} \exp \left[\frac{i}{\hbar} \mathbf{p} \cdot \mathbf{r} - \int_{t_0}^t dt' \frac{1}{2m} \left(\mathbf{p} - \frac{e}{c} \mathbf{A}(t') \right)^2 \right]. \quad (7)$$

$$\int d^3r \varphi_p^*(\mathbf{r}, t) \varphi_{p'}(\mathbf{r}, t) = \delta_3(\mathbf{p} - \mathbf{p}'), \quad \int d^3p \varphi_p(\mathbf{r}, t) \varphi_p^*(\mathbf{r}', t) = \delta_3(\mathbf{r} - \mathbf{r}'). \quad (8)$$

To solve the original problem of Eq. (6) we write the exact wave function as a superposition of an incoming Volkov state and a correction term, which vanishes at the beginning of the interaction (in the remote past $t_0 \rightarrow -\infty$). The correction term can also be expressed in terms of the Volkov states, since these form a complete set (see the equation of (8)),

$$\Psi(\mathbf{r}, t) = \varphi_{\mathbf{p}_i}(\mathbf{r}, t) + \int d^3p a_p(t) \varphi_p(\mathbf{r}, t), \quad a_p(t_0) = 0. \quad (9)$$

It is clear that the unknown expansion coefficients $a_p(t)$ describe the non-trivial transition symbolized as $\mathbf{p}_i \rightarrow \mathbf{p}$, from a Volkov state of momentum \mathbf{p}_i to another Volkov state with momentum \mathbf{p} . If we take the projection of Ψ into some Volkov state $\varphi_p(t)$ we get

$$\int d^3r \varphi_p^*(\mathbf{r}, t) \Psi(\mathbf{r}, t) = \delta_3(\mathbf{p} - \mathbf{p}_i) + a_p(t). \quad (10)$$

By inserting Ψ of Eq. (9) into the complete Schrödinger equation (6), we receive the following integro-differential equation for the coefficients $a_p(t)$,

$$i\hbar\dot{a}_{p'}(t) = \int d^3r\varphi_{p'}^*(\mathbf{r}, t')U(\mathbf{r})\varphi_{p_i}(\mathbf{r}, t') + \int d^3pa_p(t) \int d^3r\varphi_{p'}^*(\mathbf{r}, t')U(\mathbf{r})\varphi_p(\mathbf{r}, t'), \quad (11)$$

where the scalar product was taken with $\varphi_{p'}(t)$ on both sides of the resulting equation and the orthogonality property of the Volkov states was taken after all (see the first Eq. of (8)). Owing to the initial condition $a_p(t_0) = 0$, displayed already in (8) the formal solution of (6) can be written as

$$a_{p'}(t) = -\frac{i}{\hbar} \int_{t_0}^t dt' \int d^3r\varphi_{p'}^*(\mathbf{r}, t')U(\mathbf{r})\varphi_{p_i}(\mathbf{r}, t') - \frac{i}{\hbar} \int_{t_0}^t dt' \int d^3pa_p(t') \int d^3r\varphi_{p'}^*(\mathbf{r}, t')U(\mathbf{r})\varphi_p(\mathbf{r}, t'). \quad (12)$$

In the spirit of the iteration procedure used in scattering theory the $(k+1)$ -th iterate of $a_p(t)$ is expressed by the k -th iterate on the right hand side in (12) like

$$a_p^{(k+1)}(t) = -\frac{i}{\hbar} \int_{t_0}^t dt' \int d^3r\varphi_{p'}^*(\mathbf{r}, t')U(\mathbf{r})\varphi_{p_i}(\mathbf{r}, t') - \frac{i}{\hbar} \int_{t_0}^t dt' \int d^3pa_p^{(k)}(t') \int d^3r\varphi_{p'}^*(\mathbf{r}, t')U(\mathbf{r})\varphi_p(\mathbf{r}, t'). \quad (13)$$

In the first Born approximation (where the transition amplitude is linear in the scattering potential $U(\mathbf{r})$) we receive the transition amplitude in the form

$$T_{fi} = \lim_{t \rightarrow \infty} \lim_{t_0 \rightarrow -\infty} a_{p_f}^{(1)}(t) = -\frac{i}{\hbar} \int_{-\infty}^{\infty} dt' \int d^3r\varphi_{p_f}^*(\mathbf{r}, t')U(\mathbf{r})\varphi_{p_i}(\mathbf{r}, t'). \quad (14)$$

The A^2 term drops out from the transition matrix element (14), because it represents a uniform time-dependent phase. By taking the explicit form of the Volkov states (7) with the vector potential $A(t) = \mathbf{e}A_0\cos(\omega t)$ and T_{fi} becomes

$$T_{fi} = \sum_{n=-\infty}^{\infty} T_{fi}^{(n)}, \quad T_{fi}^{(n)} = -2\pi i \delta \left(\frac{p_f^2 - p_i^2}{2m} + n\hbar\omega \right) J_n(z) \frac{U(\mathbf{q})}{(2\pi\hbar)^3}, \quad (15)$$

before the time integration was done, the exponential expression was expanded into a Fourier series with the help of the Jacobi-Anger formula [26] which gave us the Bessel function

$$e^{iz\sin(\omega t)} = \sum_{n=-\infty}^{\infty} J_n(z)e^{in\omega t}. \quad (16)$$

The $U(\mathbf{q})$ is the Fourier transform of the scattering potential with the momentum transfer of $\mathbf{q} \equiv \mathbf{p}_i - \mathbf{p}_f$ where \mathbf{p}_i is the initial and \mathbf{p}_f is the final electron momenta its absolute value is $q = \sqrt{p_i^2 + p_f^2 - 2p_i p_f \cos(\theta_{p_i, p_f})}$. In our case, for 0.1 -1 eV energy electrons in the $n = 0$ channel the following approximation is valid $q \approx 2p_i |\sin(\theta/2)|$.

In general the Dirac delta describes photon absorptions ($n < 0$) and emissions ($n > 0$). $J_n(z)$ is the Bessel function with the argument of containing the relevant informations about the laser field, the intensity and the frequency $z \equiv \frac{2a_0 q \sin(\theta/2) \cos(\chi)}{\hbar\omega/c}$ where a_0, q, χ are the dimensionless intensity parameter, the momentum transfer of the electron and the angle between the momentum transfer and the polarization direction of the EM field, respectively.

The final differential cross section formula for the laser assisted collision with simultaneous n -th-order photon absorption and stimulated emission processes are

$$\frac{d\sigma^{(n)}}{d\Omega} = \frac{p_f}{p_i} J_n^2(z) \frac{d\sigma_B}{d\Omega}. \quad (17)$$

The $\frac{d\sigma_B}{d\Omega} = \left(\frac{m}{2\pi\hbar^2}\right)^2 |U(\mathbf{q})|^2$ is the usual Born cross section for the scattering on the potential $U(r)$ alone (without the external EM field). The expression Eq. (17) was calculated by several authors using different methods [6–13]. Note, that if the Born cross section is exactly known Eq. (17) can be substituted in Eq. (3) and the single-particle lifetime can be easily calculated.

C. Scattering model potentials in semiconductors

Different kind of analytic model potentials are available to model electron scattering on impurities in a semiconductor. The simplest model is the usual "box potential" which is well-known from quantum mechanics. It is capable to mimic the two-dimensional impurity scattering provide by a cylindrical-barrier of radius a . It can be used to describe a neutral impurity such as the Al atom that has diffused from a barrier into GaAs well [3]. $U(r) = U_0$ if $r \leq a$ and $U(r) = 0$ if $r > a$ where U_0 is the depth of the square well potential in eV and a is the radius in nm. The two dimensional Fourier transformation of the potential gives us the first-order Bessel function of the form of $U(q) = \pi a^2 U_0 \frac{J_1(2qa)}{qa}$.

The infinite range Coulomb potential has an infinite total scattering cross section in the first-order Born approximation, however considering a maximal limiting impact parameter due to electron screening in semiconductor the isotropic elastic cross section can be evaluated Eq. (3). This is the advent of impurity scattering in semiconductors done by Cornwell and Weisskopf in 1950 [22]. The second model potential is the screened Coulomb potential (also known as the Yukawa potential) in solid-state physics called the Brooks-Herring(BH) model [23, 24] and applicable to describe electron scattering an an ionized impurity atom

$$U(r) = \frac{\varepsilon e^{-r/\lambda_D}}{4\pi\epsilon_0\epsilon_r r}, \quad (18)$$

where $\lambda_D = \sqrt{\frac{\epsilon_0\epsilon_r k_B T}{q^2 n_0}}$ is the Debye screen length and ϵ_0, ϵ_r are the vacuum and the media dielectric constant, (to avoid confusion ε is used for the charge of the ionized impurity atom instead of q which is fixed for the momentum transfer of the electrons). The Fourier transform of this potential is as follows

$$U(q) = \frac{\varepsilon^2 \lambda_D^2}{\epsilon_0 \epsilon_r (1 + q^2 \lambda_D^2)}. \quad (19)$$

Details of the calculation can be found in the book of [2]. Beyond this phenomenological consideration more realistic screening lengths can be calculated with the Friedel sum and the phase shift analysis of the potential [21]. There are numerous models available from the original BH interaction which include various type of additional effects like, dielectric of Thomas-Fermi screening, electron-electron interaction and so on [21]. The original BH can be calculated from a realistic electron concentration of the ionized impurity containing the Fermi-Dirac integral [25] as well.

There are two additional potentials which are widely used to model impurities in semiconductors. The first has been developed to investigate be the electron charged dislocation scattering in an impure electron gas. The derivation of the formula can be found in [1]. The radial potential has the form of $U_r = \frac{\epsilon}{2\pi\epsilon_r c} K_0\left(\frac{r}{\lambda_D}\right)$ where K_0 is the zero-order modified Hankel function, $\epsilon, \epsilon_r, 1/c, \lambda_D$ are the elementary charge, dielectric constant, line charge density and the Debye screening length. Note, that as a dislocation it is a two dimensional interaction and has a cylindrical symmetry. The Fourier transformed potential has the form of $U(q) = \frac{\epsilon\lambda^2}{\epsilon_r c(1+q^2\lambda^2)}$. With this interaction Jena [27] evaluated the quantum and classical scattering times due to charged dislocation in an impure electron gas. Half a century earlier Pödör [28] calculated and analytic formula for relaxation time and investigated the electron mobility in plastically deformed germanium. Note, the remarkable equivalence to the three dimensional Yukawa potential.

The last model is the most advanced, namely dipole scattering in polarization induced two-dimensional electron gas considering the electrical field of a dipole above a plane. Additional technical details can be found in the paper of [29]. The Brooks-Herring models will be deeply analyzed in the following.

D. Generalized field assisted potential scattering in a media

The outlined laser assisted potential scattering description with the listed potentials is not sufficient for a realistic model to evaluate electron conduction in a solid at finite temperature. We consider two additional improvements.

Firstly, the scattering electrons move in a media (now in a doped semiconductor) instead of vacuum, therefore the answer of the media, the dielectric response functions has to be taken into account. We modify Eq. (17) and include

the numerically evaluated Lindhard dielectric function [30] in the scattering potential. It can be shown with the help of the quantum Vlasov theory in the first Born approximation using the Wigner representation of the density matrix of the electron [32] that in the frequency domain the total interaction potential is equivalent to the Fourier transformed interaction potential in vacuum multiplied by the Lindhard dielectric function. Therefore our final angular differential cross section formula reads

$$\frac{d\sigma^{(n)}}{d\Omega} = \frac{p_f}{p_1} \left(\frac{m}{2\pi\hbar^2} \right)^2 J_n^2(z) |U(\mathbf{q}, \epsilon_r[k, \omega])|^2, \quad (20)$$

note that the dielectric function now depends on the angular frequency of the external applied field (in our case the coherent IR field) and the wave vector of the scattering electron. The correct form of the interaction for the Brooks-Herring model is the following:

$$U(q, k, \omega) = \frac{\varepsilon^2 \lambda_D^2}{\epsilon_0 \epsilon_r(k, \omega) (1 + q^2 \lambda_D^2)} \quad (21)$$

remembering that the ε in the nominator is the charge of the impurity. The next step is to calculate the Lindhard dielectric function. For a fermion gas with electronic density n and finite temperature T a useful form is expressed in terms of real and imaginary part [33]

$$\varepsilon_r(k, \omega) = \varepsilon_{rR}(k, \omega) + i\varepsilon_{rI}(k, \omega). \quad (22)$$

At finite temperature the dielectric function contains singular integrals of the Fermi function which can be eliminated with various mathematical transformations. According to [34] the following expressions have to be evaluated:

$$\varepsilon_{rR}(k, \omega) = 1 + \frac{1}{4\pi k_F \kappa^3} [g_t(\lambda_+ = u + \kappa) - g_t(\lambda_- = u - \kappa)], \quad (23)$$

and

$$\varepsilon_{rI}(k, \omega) = \frac{t}{8k_F \kappa^3} \ln \left[\frac{1 + \exp(\alpha(t) - \lambda_-^2)/t}{1 + \exp(\alpha(t) - \lambda_+^2)/t} \right]. \quad (24)$$

Where the Fermi wave vector is $k_F = [3\pi^2 n]^{1/3}$, the reduced temperature is $t = T/T_F$, the Fermi energy is $E_F = k_F^2/2 = k_B T_F$. The reduced variables u and κ introduced by Lindhard are defined as

$$u = \frac{\omega}{v_F k}, \quad \kappa = \frac{k}{2k_F}, \quad (25)$$

where ω means the angular frequency of the IR field and k is the wave vector or the scattered electron in our model. At first the reduced chemical potential $\alpha(t) = \mu/E_f$ has to be evaluated at finite temperature from the integral of

$$\int_0^{+\infty} x^2 \frac{1}{1 + \exp(\frac{x^2 - \alpha(t)}{t})} dx = \frac{1}{3}. \quad (26)$$

With the knowledge of the chemical potential the function $g_t(\lambda)$ can be evaluated via an integral where the usual singularity is successfully eliminated by a mathematical transformation

$$g_t(\lambda) = \lambda^2 \int_0^{+\infty} \left[-2A \frac{X \exp(AX^2 - B)}{1 + \exp(AX^2 - B)^2} \right] \times \left[-X + \frac{1 - X^2}{2} \ln \left| \frac{X + 1}{X - 1} \right| \right] dX. \quad (27)$$

where $A = \lambda/t$ and $B = \alpha(t)/t$. Additional technical details, which we now neglect can be found in the original paper [34].

At this point we mention that the static $\epsilon(q, \omega \rightarrow 0)$ and the long wavelength limit $\epsilon(q \rightarrow 0, \omega)$ of the Lindhard function can be reduced to analytic formulas [30, 31]. For the static limit $\epsilon(q, 0) = 1 + \frac{\kappa^2}{q^2}$ here, κ is the 3D screening wave number (3D inverse screening length) defined as $\kappa = \sqrt{\frac{4\pi e^2}{\varepsilon} \frac{\partial n}{\partial \mu}}$. Where n, μ, ε are the particle density N/L^3 , chemical potential and the charge. However, in the long wavelength limit in 3D we get $\epsilon(0, \omega) = 1 - \frac{\omega_{plasma}^2}{\omega^2}$ where the angular frequency of the plasma reads $\omega_{plasma}^2 = \frac{4\pi e^2 N}{\varepsilon L^3 m}$.

Secondly, at finite temperature in a realistic semiconductor the scattering electrons are far from being monochromatic, therefore an averaging over the distribution has to be evaluated

$$\langle G \rangle = \frac{e^2}{m^* n_{imp}} \langle \tau \rangle. \quad (28)$$

This means an additional numerical integration of the relaxation time multiplied by the Fermi-Dirac distribution function $f(E)$ (for non-degenerate electrons) times the density of states $g(E)$ according to Shang [2]

$$\langle \tau \rangle = \frac{\int_0^\infty \tau(E) f(E) g(E) dE}{\int_0^\infty f(E) g(E) dE} \quad (29)$$

with $E(k) = \frac{\hbar^2 k^2}{2m}$ being the energy of the electrons. In this representation the integration can be traced back to an integral over k . The numerical value of the density of state function is well-known for one, two or three dimensional solids. For a two dimensional system $g(E)_{2D} = \frac{m_e}{2\pi\hbar^2}$ it is independent of the electron energy in three dimension (which is our present Brooks-Herring potential case) however $g(E)_{3D} = \frac{m_e^{3/2}}{\sqrt{2\pi^2\hbar^2}} \sqrt{E}$. (The mentioned charged dislocation potential is a two dimensional model.)

If the number of donors are enhanced, the Fermi level will rise more and more towards the conduction band. At some stage the approximations will no longer hold because more than only the tail of the Fermi Dirac function overlaps with the band edge. The approximations break down when the Fermi level gets closer than about $3k_B T$ to one of the band edges. At room temperature this is approximately 75 meV. In that case the semiconductors become degenerate and the Boltzmann distribution function has to be taken instead of the Fermi-Dirac one.

In practical calculations the upper limit of the integral can be cut at the Fermi energy which is about 1eV at room temperature for semiconductors. Numerical values obtained from (29) with or without external electromagnetic field can be directly compared in the future to experimental data.

III. RESULTS

We consider doped semiconductors with Fermi energy of one eV. Therefore as external field we take coherent IR electromagnetic sources with the wavelength in the range of one to ten microns. It is well-known [35] that CO₂ lasers have numerous lines between 4.32 and 17.37 μm . It is worth to mention that the last decade far infrared THz laser lines were created from methylene isomers pumped with CO₂ lasers [36, 37] with intensities of hundred mW.

As maximal intensities we take $10^{12} < I < 5 \cdot 10^{14} \text{ W/cm}^2$. For instance, such sources will be available in the not-so far future in the ELI ALPS. According to ref. [21] half a dozen electron mobility versus electron concentration measurement were presented and compared to various BH models on a logarithmic-linear scale below 200 K giving discrepancy of a factor of 2-5.

As lowest level of the kinetic energy of the electrons we consider the thermal noise $E = k_B T$ which is 0.025 eV at room temperature. The parameters of the BH potential are the following $\lambda_d = 30 \text{ nm}$, $\epsilon_r = 35$, $\epsilon = 1$ Unusual to solid state studies and similar to atomic or nuclear physics Fig. 1 presents the integrand of the total cross sections Eq.(3) for three different model calculations. The energy of the scattered electron is 0.1 eV. The solid black line presents the pure electron scattering on the BH potential Eq.(19), it has a simple decaying structure for large back-scattering angles. The red long-dashed line is for BH potential multiplied by the Bessel function according to Eq.(17), note that a numerical dielectric constant was used $\epsilon_r = 35$. The wavelength and intensity of the external field are $\lambda = 3\mu\text{m}$ and $I = 10^{14} \text{ W/cm}^2$.

The third, the blue short-dashed line presents the laser assisted scattering Eq.(17) where the frequency and electron wave-vector dependent Lindhard function was included Eq.(21). It is clear that radical enhancement of the cross section is due to the Lindhard function. The shape of such angular-dependent cross sections are well-known in nuclear [16, 17] and atomic physics with the numerous local flat maxima and sharp minima. Note, that the cross sections are finite at the minima with non-existing derivatives.

The magnitude of the angular differential cross section is in the range of $10^{-11} \mu\text{m}^2$ which is about 10^{-18} cm^2 .

Evaluating the angular integral of Eq. (3) for 0.1 eV electron energy we got the three total cross section values of $\sigma_1 = 2 \cdot 10^{-18} \text{ cm}^2$, $\sigma_2 = 1.1 \cdot 10^{-18} \text{ cm}^2$, which are 2 and 1.1 megabarn. The third cross section is $\sigma_3 = 1.4 \cdot 10^{-15} \text{ cm}^2$. It is clear to see that the integrand of Eq.(17) or Eq.(21) strongly depend on the energy (or impulse) of the scattering electron. The shape of the functions in Fig. 2 are similar but the magnitude are different for different electron momenta. It is important to emphasize, that the presented functions on a linear-logarithmic scale looks sometimes illusory, large discrepancies between the running lines may become just a tiny difference after an integration process. The BH scattering potential is not singular at $k \rightarrow 0$ zero electron momenta, however the absolute valued Lindhard

function square $|\epsilon(k=0, \omega)|^2$ is singular at the origin. It can be shown with Eq. (23), Eq. (24) and Eq. (21) that the final interaction potential goes to zero at zero electron momenta, which meets our physical consideration. If we want to evaluate the effect of the external IR field on the cross sections and later on the electric conduction to have physically measurable data then an additional integral over the electron momenta is needed averaged over the Fermi distribution as mentioned above Eq. (29). Fig. 3 shows us the integrand of the nominator of Eq. (29). The main contribution of the integral comes from low energy electrons, the additional Fermi function smooths out the narrow minima and not to see on the figure.

The numerical value of this integral for the pure BH potential is 0.000875373. The dimension of the number will be analysed a bit later. Tab I, II, and III. shows us the final numerical value of the mean value of the relaxation time for various external IR field intensities and wavelength. The third column of the tables contain the values where the $\epsilon_r = 35$ numerical dielectric constant was used, the fourth column contain the values where the field-dependent Lindhard function was applied. The dimension of the calculated values is $s/\mu m^2$. Multiplying with the remaining constants of $\frac{e^2}{m^* n_{imp}}$ where the charge of the electron is $1.6 \cdot 10^{-19} C$ the effective mass of an electron in a semiconductor is about $0.5 \times 9.0 \cdot 10^{-31}$ kg and the number of the impurities per cm^3 lies between $10^9 - 10^{16}$ therefore the obtained final conductance values would lie between $10^{-6} - 10^5$ Si/cm [38]. Therefore we do not give exact numerical conductance values, (not a specific material was analyzed) we just want to emphasize that the ratio of the conductances with or without strong external IR fields can vary drastically. The first message is the following, if no additional frequency dependent dielectric function is taken into account (which is not probable, that is the simplest model) then the strong IR fields may cause a factor of 4 enhancement of the resistivity (inverse conductivity) for $6 \mu m$ wavelength and a factor of almost ten for $9 \mu m$ wavelength. This is already a considerable difference which may attract the interest of experimentalists. Another, more important message is that a more sophisticated model, (including frequency dependent dielectric function) may give a controversy, an even vehement change of the conductance. For $3 \mu m$ wavelength there is a factor of 614 reduction of the resistivity. At $6 \mu m$ wavelength the factor is about 90, and for $9 \mu m$ the argument reduces to a factor of 27. For these three wavelengths the larger the field intensity the larger the change of the resistivity due to the enhancing argument of the Bessel function. The intensity dependence of the resistivity variation is very low at these values. We checked, and found that at much lower intensities like $I = 10^7 - 10^8 W/cm^2$ the reduction of the change goes to zero.

A doped semiconductor has a complex nature and the physical value of the resistivity change in an external IR field can of course only be investigated in a real physical experiment but our calculation shows that it would be an interesting project.

These are all scattering processes, without any photon absorption. If we include one photon absorption the zeroth order Bessel function has to be changed to the first order one, otherwise the process and the way of calculation remains the same. In general the cross sections and the obtained conductances became three magnitude lower for the mentioned wavelength and intensities.

The two-fold numerical integrations of Eq. (29) for various laser parameters were evaluated with Wolfram Mathematica [Copyright 1988 – 2012 Wolfram Research, Inc.] where the global adaptive integration built-in method was used with recursion number of 300, additionally the numerical precision was set up to ten digits.

| Laser intensity [W/cm^2] | Wavelength $\lambda[\mu m]$ | $\langle \tau \rangle$ Eq. (29) with Eq. (19)) | $\langle \tau \rangle$ Eq. (29) with Eq. (21) |
|---------------------------------|--------------------------------|---|--|
| 10^{11} | 3 | 0.0008751 | 0.5398931 |
| 10^{12} | 3 | 0.0008653 | 0.5342114 |
| 10^{13} | 3 | 0.0008558 | 0.5298223 |
| 10^{14} | 3 | 0.0008463 | 0.5248491 |

Table 1. The results for the BH potential for various field intensities.

| Laser intensity [W/cm^2] | Wavelength $\lambda[\mu m]$ | $\langle \tau \rangle$ Eq. (29) with Eq. (19)) | $\langle \tau \rangle$ Eq. (29) with Eq. (21) |
|---------------------------------|--------------------------------|---|--|
| 10^{11} | 6 | 0.0002151824 | 0.078952 |
| 10^{12} | 6 | 0.000213123 | 0.078935 |
| 10^{13} | 6 | 0.000211618 | 0.078772 |
| 10^{14} | 6 | 0.000207095 | 0.078006 |

Table 1. The relaxation time for the BH potential for various field intensities.

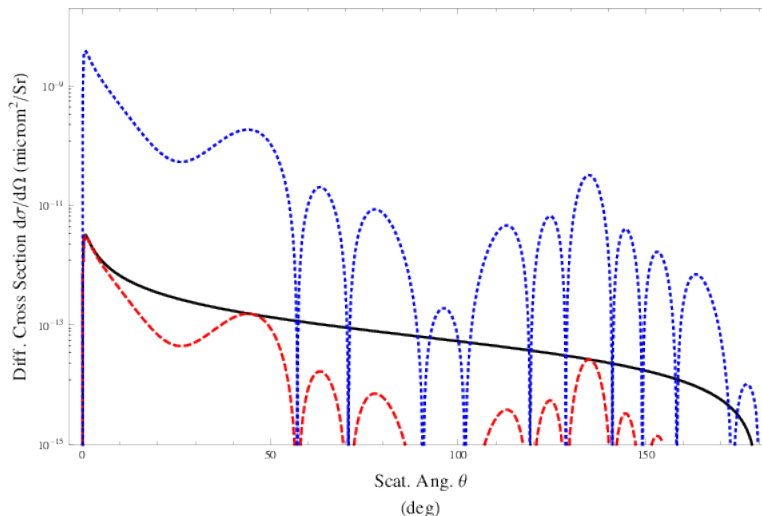


FIG. 2: The differential cross section Eq.(3), the black solid line is for the pure electron scattering on the BH potential Eq.(19), the red long-dashed line is for BH potential multiplied by the Bessel function according to Eq.(17) and the blue short-dashed line is for the Lindhard corrected BH potential Eq.(21) inserted into Eq.(17). The wavelength is $\lambda = 3\mu\text{m}$ and the intensity is $I = 10^{14} \text{ W/cm}^2$.

| Laser intensity [W/cm^2] | Wavelength $\lambda[\mu\text{m}]$ | $\langle\tau\rangle$ Eq. (29) with Eq. (19) | $\langle\tau\rangle$ Eq. (29) with Eq. (21) |
|--|--------------------------------------|--|--|
| 10^{11} | 9 | 0.0000972694 | 0.032594 |
| 10^{12} | 9 | 0.0000969269 | 0.030221 |
| 10^{13} | 9 | 0.0000962693 | 0.028563 |
| 10^{14} | 9 | 0.0000958826 | 0.024270 |

Table 1. The results for the BH potential for various field intensities.

IV. SUMMARY

We presented a formalism based on an interrelated model to calculate electron conductance in a doped semiconductor in strong external IR fields. We coupled the mathematical description of multi-photon processes to the well-established potential scattering model based on the first-Born approximation. As an application of our general formalism in the present paper the emphasis has been put on the modification of the scattering elastic cross sections in the elastic channel. In solid state physics the elastic scattering of electrons on impurities modeled by the Brooks-Hering potential can model the electric conductance up to a factor of ten which is a reliable background [21]. We treated the electron scattering in a perturbative manner, the influence of the external strong radiative IR field (which can cause photon absorption) is however treated non-perturbatively. Closer to future possible experiments we improved the solid state scattering model on two points. First, instead of the static dielectric constant, which models the semiconductor itself we included a frequency dependent Lindhard function which mimics the response of the solid to a quick varying external field. This improvement of the model gave us at least a factor of two (or even two magnitudes at other wavelength) in the final numerical conductance values. As a second point, to come closer to nature, we average over the final electron energy distribution above the Fermi function at room temperature. In some cases (when no realistic Lindhard model was applied) this phenomena smooth out the gain due to the external field. We have demonstrated that owing to the joint interaction of the conduction electrons with the impurity scattering potential and the laser field, there could be a considerable change in the conduction as we have expected at the beginning of our studies. Our theoretical results will stimulate future experiments in ELI-ALPS which might open the way to a new kind of quick gating instrument.

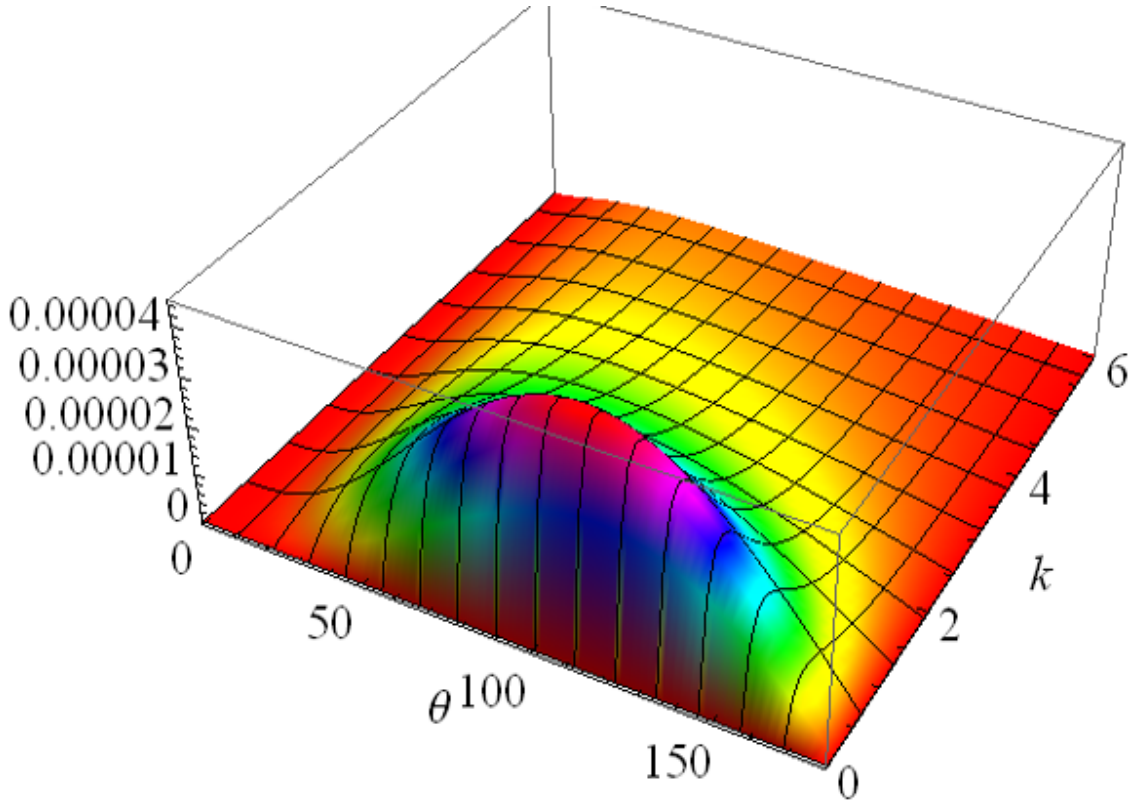


FIG. 3: The two-dimensional integrand of the nominator of the averaged relaxation time Eq. (29) where $\lambda = 3\mu\text{m}$, and $I = 10^{14}$ W/cm^2 . Note, that due to the Fermi function the numerous finite singularities presented on Fig. 2. is smoothed out and not to see.

V. ACKNOWLEDGEMENT

We thank for Dr. Ugo Ancarani and Mr. András Pocsai for useful discussion about numerical problems arose calculating Lindhard function. The ELI-ALPS project (GINOP-2.3.6-15-2015-00001) is supported by the European Union and co-financed by the European Regional Development Fund.

-
- [1] K. Seeger, *Semiconductor Physics*, Springer 2004.
 - [2] S. Li Sheng, *Semiconductor Physical Electronics*, Springer 2006.
 - [3] J. H. Davies, *The Physics of Low-Dimensional Semiconductors*, Cambridge University Press 1998.
 - [4] J. Sólyom, *Fundamentals of the Physics of Solids*, Springer 2010.
 - [5] A. Di Piazza A, C. Müller, Z.K. Hatsagortsyan and C.H. Keitel, *Rev. Mod. Phys.* **84**, 1171 (2012).
 - [6] F.V. Bunkin and M.V. Fjodorov, *ZsETF* **49**, 1215 (1965).
 - [7] F.V. Bunkin, M.V. Fjodorov and A. E. Kazakov, *Usp. Fiz. Nauk.* **107**, 559 (1972).
 - [8] F.H.M. Faisal, *Phys. B. Atom. Mol. Phys.* **6**, L312 (1972).
 - [9] N.M. Kroll and K.M. Watson, *Phys. Rev. A* **8**, 804 (1973).
 - [10] Y. Gontier and N.K. Rahman, *Lett. al Nuovo Cim.* **9**, 537 (1974).
 - [11] J. Bergou, *Phys. A: Math. Gen.* **13**, 2817 (1980).
 - [12] J. Bergou and S. Varró, *Phys. A: Math. Gen.* **13**, 2823 (1981).
 - [13] F.H.M. Faisal, *Theory of Multiphoton Processes*, Plenum Press, 1987.
 - [14] F. Ehlötzky, A. Jaron and J.Z. Kaminsky, *Phys. Rep.* **297**, 63 (1998).
 - [15] R. Kanya and K.Yamanouchi, *Phys. Rev. A* **95**, 033416 (2017).
 - [16] I.F. Barna and S. Varró, *Laser and Part. Beams* **33**, 299 (2015).
 - [17] I.F. Barna and S. Varró, *Nucl. Instr. and Meth. in Phys. Res. B* **369**, 77 (2016).
 - [18] M. Schultze *et al.* *Science*, **346**, 1348 (2014).
 - [19] M.S. Wismer *et al.* *Phys. Rev. Lett.* **116**, 197401 (2016).

- [20] <http://www.eli-alps.hu>.
- [21] D. Chattopadhyay and H.J. Queisser, *Rev. Mod. Phys.* **53**, 745 (1981).
- [22] E. Conwell and V.F. Weisskopf, *Phys. Rev.* **77**, 388 (1950).
- [23] H. Brooks, *Phys. Rev.* **83**, 879 (1951).
- [24] C. Herring and E. Vogt, *Phys. Rev.* **101**, 944 (1956), *ibid.* **105**, 1933 (1957).
- [25] R.B. Dingle, *Philos. Mag.* **46**, 831 (1955).
- [26] M. Abramowitz and I. Stegun, *Handbook of Mathematical Functions* Dover Publication., Inc. New York 1968 Chapter 9, Page 368. Eq. 9.2.1.
- [27] D. Jena and U.K. Mishra, *Phys. Rev B.* **66**, 241307(R) (2002).
- [28] B. Pödör, *Phys. Stat. Sol.* **16**, K167 (1966).
- [29] D. Jena, A.C. Gossard and U.K. Mishra, *J. Appl. Phys.* **88**, 4734 (2000).
- [30] J. Lindhard, *Dan. Mat.-Fys. Medd.* **28**, 1 (1954).
- [31] N.W. Ashcroft and N.D. Mermin, *Solid State Physics*, Thomson Learning, Toronto 1976.
- [32] H.J. Kull and L. Plagne, *Phys. Plasmas*, **8**, 5244 (2001). (Eq. 31 is considered).
- [33] N.R. Arista and W. Brandt, *Phy. Rev. A* **29**, 1471 (1984).
- [34] L.U. Ancarani and H. Jouin, *Eur. Phy J. Plus*, **131**, 114 (2016).
- [35] R. Beck . W. Englisch and K.Gürs, *Table of Laser Lines in Gases and Vapors*, Springer 1976.
- [36] L.F.L. Costa *et al.*, *Journ. Mol. Spectr.* **241**, 151 (2007).
- [37] A. Moretti *et al.*, *IEEE Journ. Quant. Electr.* **44**, 1104 (2008).
- [38] O. Milton, *Engineering Material Science* Volume 1 (3rd ed) p. 561, Academic Press 1995.